Navigation of Mini Swimmers in Channel Networks with Magnetic Fields*

Fatma Zeynep Temel, Ayse Ecem Bezer, and Serhat Yesilyurt, *Member, IEEE*

***Abstract*— Controlled navigation of swimming micro robots inside fluid filled channels is necessary for applications in living tissues and vessels. Hydrodynamic behavior inside channels and interaction with channel walls need to be understood well for successful design and control of these surgical-tools-to-be. In this study, two different mechanisms are used for forward and lateral motion: rotation of helices in the direction of the helical axis leads to forward motion in the viscous fluid, and rolling due to wall traction results with the lateral motion near the wall. Experiments are conducted using a magnetic helical swimmer having 1.5 mm in length and 0.5 mm in diameter placed inside two different glycerol-filled channels with rectangular cross sections. The strength, direction and rotational frequency of the externally applied rotating magnetic field are used as inputs to control the position and direction of the micro swimmer in Y- and T-shaped channels.**

I. Introduction

Experimental and theoretical studies on swimming micro robots receive much attention in recent years due to their great potential in medical applications. The use of bio-inspired micro swimmers for tasks like destroying blood clots in clogged arteries or targeted drug delivery will be advantageous in minimally invasive surgical procedures [1]. Nonetheless, development of micro-motors inspired by actuation mechanisms of natural micro swimmers moving in fluidic environments with helical flagella is very difficult [2, 3]. However, application of external magnetic fields to render forces and torques on magnetic micro robots for propulsion is a promising alternative; Helmholtz coils [4, 5, 6] and permanent magnets [7] are used to induce external magnetic fields.

Swimming mechanisms using planar and helical wave propulsion are used in experiments to demonstrate bio-inspired micro swimmers moving with the help of externally applied magnetic fields [8, 9, 10, 11]: the commonly used propulsion mechanism for micro swimmers is the rotation of helical tails, since rotating magnetic fields can easily be generated [12]. For instance, artificial bacterial flagella are manufactured from GaAs by Zhang et al., measured as 1.8 μm in width, 30μm in length, 200 nm in thickness and attached to a soft magnetic nickel on one side [13, 14]. Authors demonstrated that the flagella swim along its helical axis with the externally applied rotating magnetic field in that direction obtained by electromagnetic coil pairs, and concluded that size of the head and strength of the applied magnetic field affect the linear swimming velocity. In addition, 3D steering of helical micro swimmers is accomplished by a low-strength, rotating magnetic field with micrometer positioning precision inside a water filled tank [13, 14]. Another study on swimming micro structures was carried out by Ghosh and Fisher [15], who manufactured and operated chiral colloidal propellers having 200-300 nm width and 1-2 μm length: swimmers were made of silicon dioxide and a thin layer of ferromagnetic material (cobalt) was deposited on one side. Rotational magnetic fields were used to navigate the magnetic nano-structured propellers in water with micrometer level precision [15].

Furthermore, two new methods of manufacturing robots with helical tails are tested. First is the construction of 8.8μm long micro carriers that consist of micro holders and helical structures using 3D laser processing and physical vapor deposition [16]. Tottori et al. coated micro carriers with two thin Ni/Ti layers using electron beam evaporator, so that the micro machines are controlled with the aid of externally applied magnetic fields [16]. Second is the coating of liposomes, which have self-formed two-layered spiral structures or tubules, by CoNiReP in order to obtain rigid and magnetically controllable structures [17]. The motion of these helices was than observed under a 5 DOF system that consists of eight electromagnets [17].

Experiments using cm-sized robots that consist of helical structures wound around on a body and setups that consist of electromagnetic coil combinations to control and navigate the helical swimmers are reported in literature [18, 19]. For instance, Mahoney et al. [20] manufactured a screw like robot having 5.6 mm length and 1.4 mm diameter and investigated its motion inside a soft tissue. Unstable motion of robots is observed when the rotational frequency of applied magnetic field exceeds a certain value [20] similar to [13, 14, 15].

In-channel experiments are significant for their relevance to applications of micro robots inside living organisms. A cm-long spiral swimming robot is actuated by Honda et al. [21] using external rotating magnetic field to obtain propagation in a silicon-oil-filled, 15-mm-diameter channel. Authors showed that motion of the robot has a linear relationship with the excitation frequency. Hydrodynamic interactions between swimming organisms and solid surfaces were investigated by Berke et al. [22] by measuring the distribution of E.coli swimming between glass plates and results were compared with a hydrodynamic model. Another study about bacteria swimming near solid surfaces was conducted by Giacché et al. [23] using a boundary element method based model to predict the near-wall motion of

*Research supported by TUBITAK (The Scientific and Technological Research Council of Turkey) under the grant number 111M376.

Authors are with the Faculty of Natural Sciences and Engineering, Sabanci University, Orhanli, Tuzla, 34956 Istanbul, Turkey.

(e-mail: zeyneptemel@sabanciuniv.edu, aebezer@sabanciuniv.edu, syesilyurt@sabanciuniv.edu).

Preprint submitted to 2013 IEEE International Conference on Robotics and Automation. Received September 17, 2012.

flagellated microorganisms and validated their model with a set of experiments with E.coli. Recently, we conducted experiments using one-link micro robots which consist of two parts: a permanent magnet $Nd_2Fe_{14}B$ body (~360 μm in diameter) and a metal helical wire (~110μm diameter) [24]. These structures are rotated inside glycerol filled glass channels of 1-mm inner-diameter by the externally applied rotating magnetic field driven by two Helmholtz coil pairs. Up to a step-out frequency, it is observed that there is a proportional relationship between the time-averaged velocity and the rotation frequency, after which robots lose sync with the magnetic field and forward velocities drop rapidly. As the magnetic field strength is increased, it is possible to reach higher step-out frequencies, similar to the results reported in literature [13, 14].

In this study, controlled navigation of mm-sized swimmers are studied using two motion mechanisms of rotating helical structures: moving forward in fluids at low Reynolds numbers and rolling sideways due to traction forces near walls. Experiments are conducted using a magnetic micro swimmer having 1.5 mm length and 0.5 mm diameter placed inside three different glycerol-filled channels with rectangular cross sections. The strength, direction and rotational frequency of the externally applied magnetic field are controlled to move the helical swimmer forward and laterally in Y- and T-shaped channels.

II. Methodology

In what follows, components of experimental setup are discussed: robot fabrication process and the physical parameters of the robot used in the experiments, electromagnetic coil setup that provides the rotational magnetic field, channel structures, and the control algorithm to navigate magnetic swimmers in plane.

A. Robot Fabrication

Helical swimmers moving in rotational magnetic fields are fabricated using $Nd_2Fe_{14}B$ permanent magnets and nonmagnetic cylindrical copper wires. These swimmers differ from the microorganisms since a rigid connection exists between permanent magnet (head) and copper helices (tail) unlike the coupling mechanism that natural micro swimmers have, thus head and tail rotate in the same direction unlike microorganisms.

A simple procedure is used to make right-handed helices from a thin copper wire (here, with a diameter of 0.06mm) by winding it on another thicker wire (here, with a diameter of 0.48 mm) (see Fig. 1a). Desired wavelength or the number of waves on a fixed length is adjusted by stretching the helices to deform plastically. Radially magnetized cylindrical magnets with 0.4 mm diameter and 0.5mm length are placed inside the helices, and secured with a strong adhesive. The helical swimmer used in the experiments has 2 full waves on its tail and is 1.5 mm long in total. Tail length is 1 mm and wavelength is calculated as 0.5 mm (Fig. 1b). Since permanent magnets are magnetized in the radial direction, the magnetization vector is perpendicular to the long axis of the swimmer when it is rotated with a rotating external magnetic field, which is also in the radial direction.

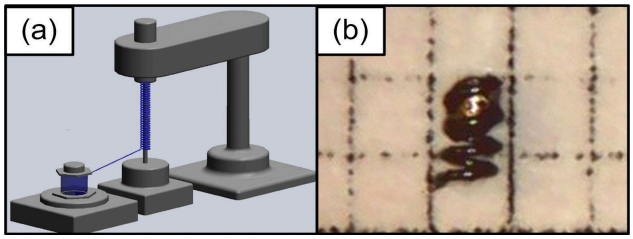

Figure 1. Helix making process (a) and the micro swimmer that consists of a permanent magnet head and a helical tail (b).

B. Experimental Setup

The magnetic helical swimmer is placed inside different channel structures in sequence. Three different channel patterns were made of acrylic glass (plexiglass) by micro machining. The Y-shaped channel (Fig. 2a) and T-shaped channel (Fig. 2b) have rectangular cross section with a cross sectional dimensions of 1.3 mm in width and 1 mm in height. Channels were then filled with glycerol, whose viscosity and density are 1.412 Pa·s and 1261 kg/m^3, respectively, at room temperature.

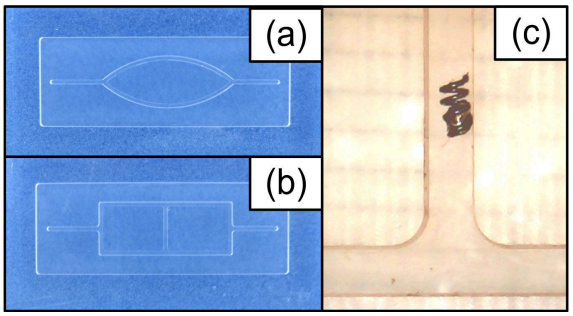

Figure 2. Channel structures with Y-shaped connections (a) and T-shaped connections (b). Millimeter size helical swimmer inside channel (c).

Helical swimmer is rotated at 1 and 5 Hz to observe different swimming modes. Reynolds number is calculated based on the forward motion of the swimmer with the diameter of the head, D_{head}, as the length scale and the velocity of the swimmer, V_{sw}, as the velocity scale, and based on the rotation of the tail with the diameter of the wire, d_{wire}, as the length and the tangential velocity of the tail, $2\pi fA$, as velocity scales, A is the amplitude; values are presented in Table 1:

$$\mathrm{Re}_{head} = \frac{\rho V_{sw} D_{head}}{\mu} \quad (1)$$

$$\mathrm{Re}_{tail} = \frac{\rho 2\pi f A d_{wire}}{\mu} \quad (2)$$

where ρ is the density, μ is the viscosity.

Preprint submitted to 2013 IEEE International Conference on Robotics and Automation. Received September 17, 2012.

TABLE I. REYNOLDS NUMBERS

	f = 1 Hz	*f = 5 Hz*
For Head	0.02×10^{-3}	13.13×10^{-3}
For Helical Tail	0.34×10^{-3}	1.68×10^{-3}

In order to control the magnetic helical robots, three electromagnetic coil pairs were placed orthogonally to obtain rotating magnetic fields (Fig. 3a) as commonly used for the propulsion and steering of helical micro swimmers as untethered swimming micro robots [12, 13, 14, 15, 21] since rotation of the helical swimmer in a viscous fluid results in the forward motion of the swimmer. The magnetic torque, τ, required to rotate a permanent magnetic particle in sync with the magnetic field is calculated from the magnetic moment, $\boldsymbol{m}$, of the particle and the magnetic induction, $\boldsymbol{B}$, of the field.

$$\tau_M = \boldsymbol{m} \times \boldsymbol{B} \tag{3}$$

The magnetic moment of the particle depends on the volume, υ, and magnetization, $\boldsymbol{M}$, of the particle.

$$\boldsymbol{m} = \boldsymbol{M}\upsilon \tag{4}$$

Helical swimmers can be propelled back and forth by using two orthogonal electromagnetic coil pairs. Third coil pair is used to control the direction of magnetic field vector and the direction of the motion of the swimmer. The frequency ($f_{x,1} = f_{x,2}$; $f_{y,1} = f_{y,2}$; $f_{z,1} = f_{z,2}$; where subscripts *x, y,* and *z* denotes the axes and *1and 2* denotes the coil number of a pair) and magnitude of the applied current ($I_{x,1} = I_{x,2}$; $I_{y,1} = I_{y,2}$; $I_{z,1} = I_{z,2}$) to the coils are the same for mutual (bilaterally placed) coils, whereas, the current applied to the orthogonally placed coils have the same frequency ($f_x = f_y = f_z$) but different current magnitude ($I_x \neq I_y \neq I_z$) to provide the same magnetic field strength ($B_x = B_y = B_z$). Besides, a phase shift exists on the supplied current between the coil pairs placed along the **z-**axis and the coil pairs placed along the **x-** and **y-**axis to generate rotational magnetic field. Helical swimmers rotate with the magnetic field vector by means of the magnetic torque on permanent magnet heads and rotate in sync with the rotating magnetic field, which results with forward motion due to the propulsion force. This method is widely used in the literature and commonly used for navigating helical swimmers in fluidic environments [12, 13, 14].

The current is transmitted to the coils from the power generators via Maxon ADS_E 50/5 4-Q-DC servo-mechanism amplifiers, each of which has a maximum current output of 10 A. Each coil is connected to one Maxon motor drive, which is connected to NI PCI-6733 high speed analog output device. The current applied to the **x-**, **y-**, and **z-**axis coils are defined as $I_x=I_{x,0}\cos(2\pi ft)$, $I_y=I_{y,0}\cos(2\pi ft)$, and $I_z=I_{z,0}\sin(2\pi ft)$, respectively. The magnitude and frequency of alternating currents are adjusted via LabView software with a joystick that is used to control the motion of the helical robots.

Motion of helical swimmers is observed with a 2.0 mega pixel CMOS digital microscope USB camera that can record maximum 30 frames per second.

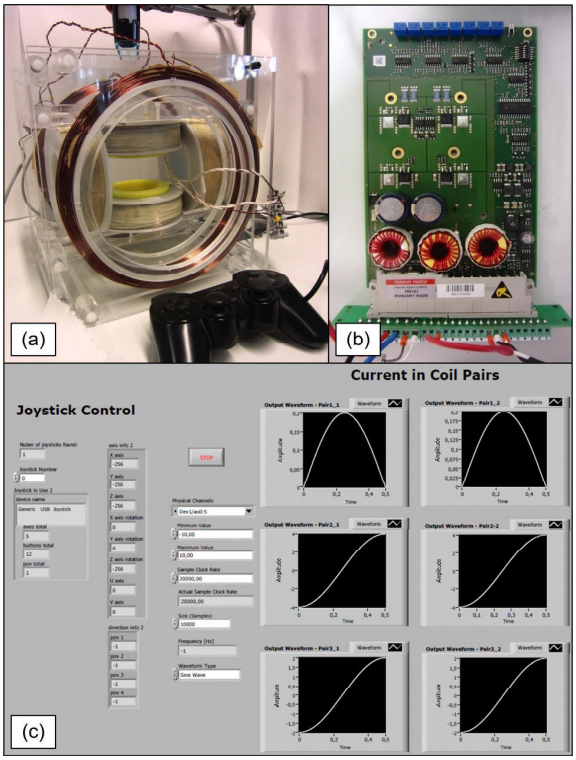

Figure 3. Experimental setup consists of othogonally placed three electromagnetic coil pairs (a) which were driven by Maxon Motor Drives (b) connected to an NI DAQ and controlled by a joystick (a) using LabView (c).

C. Controlled Navigation

Propulsion as a result of the rotation of the helical tail is a well known swimming mechanism for both natural and artificial micro swimmers. Inside rectangular channels, helical swimmers showed different swimming properties in experiments: forward motion due to the fluidic propulsion force and lateral motion due to the traction force near the solid wall. Swimmers tend to travel near solid walls due to their weight; a lift force from the wall balances the swimmer and avoids stiction to the wall and results in a very small clearance. Due to rotation, a net traction force emerges and acts as a lateral force on the robot and causes its sideways motion.

Linear and angular velocities of helical swimmers are obtained from the solution of the equation of motion. In addition to the propulsion force, traction force occurs, as well, due to the rotation of the tail when the external magnetic torque is applied. Total drag force and torque on the swimmer are as follows where subscripts *p*, *d* and *ext* denote propulsion, drag and external effects, respectively:

$$\begin{aligned} \mathbf{F}_d + \mathbf{F}_p + \mathbf{F}_{ext} &= 0 \\ \mathbf{T}_d + \mathbf{T}_{ext} &= 0 \end{aligned} \tag{5}$$

Force and torque vectors due to hydrodynamic propulsion and fluid drag are constructed by the resistive force theory [25]: the force and torque vectors are obtained

from the linear and angular velocity vectors with a linear resistance relationship as follows:

$$\begin{bmatrix} \mathbf{F}_{ext} \\ \mathbf{T}_{ext} \end{bmatrix} = \begin{bmatrix} \mathbf{F}_T \\ \boldsymbol{\tau}_M \end{bmatrix} = \left(\mathbf{C}_B + \mathbf{C}_T \right) \begin{bmatrix} \mathbf{U} \\ \boldsymbol{\Omega} \end{bmatrix} \qquad (6)$$

where, for a full six degree of freedom motion, $\mathbf{C}_B$ and $\mathbf{C}_T$ are the resistance matrices of the body and tail, respectively, $\mathbf{U}$ is the translational velocity and $\boldsymbol{\Omega}$ is the rotational velocity, $\mathbf{F}_{ext}$ is the traction force and equals $\mathbf{F}_T$, and $\mathbf{T}_{ext}$ is the magnetic torque and equals $\boldsymbol{\tau}_M$.

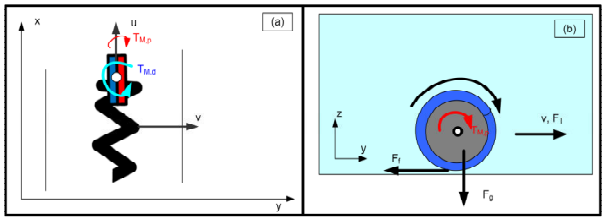

Figure 4. (a) Helical swimmer moves in positive **x**-direction with the applied positive rotational magnetic field along **x**-axis if the frequency is high. For low rotational frequencies lateral motion also occurs in positive **y**-axis. The torque for propulsion and direction is represented with $\mathbf{T}_{M,p}$ and $\mathbf{T}_{M,d}$, u is the velocity along **x**-axis and v is the velocity along **y**-axis. (b) Traction force, $\mathbf{F}_T$, due to the applied magnetic torque at low frequencies provides a velocity in lateral direction. $\mathbf{F}_f$ and $\mathbf{F}_g$ are friction and gravity forces, respectively

In addition to the longitudinal motion, because of the traction due to the channel walls, lateral motion occurs. Wall effects on a swimmer moving at low Reynolds regime is examined in [26] in detail. As a result of the channel wall, lateral motion occurs due to rotation of helical swimmer with the applied magnetic torque; equation of motion can be then written as:

$$\boldsymbol{\tau}_M = \mathbf{F}_T \cdot r = b \cdot \boldsymbol{V} = b \cdot \boldsymbol{\omega} \cdot r \qquad (6)$$

where $\mathbf{F}_T$ is the traction force, r is the radius of the helical swimmer, b is the friction coefficient, V is the lateral velocity and ω is the angular velocity of the robot.

Two types of control methods are applied to the open-loop system. On-off control is to start and stop the rotational motion of the helical swimmer; with sufficient magnetic field strength to overcome the rotational drag, swimmer can rotate with the applied frequency. Besides, swimmer can be stopped at the desired location. With appropriate position sensing systems, precise position control of the swimmer can also be performed in a closed-loop algorithm. Secondly, by changing the alignment of the magnetic field vector and the frequency of the rotating magnetic field, direction of motion is controlled. At high frequencies, robot moves along its helical axis, but the effect of the traction force cannot be observed due to dominant fluid forces. At low frequencies, because of the traction between channel wall and the swimmer, lateral force occurs and becomes dominant compared to the longitudinal motion of the swimmer.

III. Results

In what follows, results from the experiments are discussed: two different swimming modes to navigate helical swimmers inside rectangular channels, motion in Y-shaped channels, motion in T-shaped channels and the swimming (moving) strategy across an obstacle.

A. Swimming modes

At low frequencies, e.g. 1 Hz, as a result of the traction force, swimmer first moves to one side of the channel according to the rotation direction and then continues forward motion at the sideways near the channel wall whereas the forward velocity is relatively small (0.004 mm/s) (Fig. 5a).

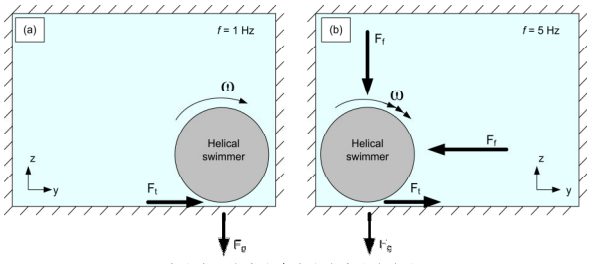

Figure 5. Motion of helical swimmer inside rectangular channel when rotational frequency, f, equals 1 Hz (a) and 5 Hz (b). In the figure, $\mathbf{F}_t$, $\mathbf{F}_g$, $\mathbf{F}_f$ and ω represent traction force, gravitational force, fluid force and angular velocity, respectively.

As the frequency increases, e.g. to 5 Hz, swimmer changes its lateral position inside the channel and begins to move toward the opposite side of the channel along with a fast forward motion reaching to a velocity of 2.94 mm/s (Fig. 5b). In order to fully understand the flow fields inside the channel due to faster rotation of the swimmer and causing the swimmer change its lateral position in the channel, a computational model is necessary. One reason for the lateral position change is the fluid force caused by the flow which is affected by the rotation. This phenomenon is similar to the one observed in [27]; although the natural micro swimmers' head and tail rotate in reverse directions in the mentioned study, at high frequencies micro organisms approach to the planar wall.

B. Navigation in Y-shaped Channel

Changing the direction of the helical swimmer is realized by changing the magnetic field vector in **xy**-plane (Fig. 6a and 6b) applied by the electromagnetic coil pairs. As explained in detail in [13], for an axially magnetized cylindrical magnetic particle, the magnetization vector is perpendicular to the long axis and follows the external magnetic field vector. The angle between two arms of Y-shaped channel is measured as 70^o at the beginning of the junction. The resultant magnetic field vector in **xy**- plane should be rotated 35^o either in positive or negative direction; depending on the way that robot is wanted to follow (Fig. 6a). In order to move the swimmer backwards, direction of the rotational frequency is altered.

Preprint submitted to 2013 IEEE International Conference on Robotics and Automation. Received September 17, 2012.

C. Navigation in T-shaped Channel

Similar to the previous case, direction of magnetic field vector is changed in the **xy**-plane to satisfy a resultant vector which is perpendicular to the desired direction of motion. In order to rotate the direction of the rotating magnetic field by 90°, the current supplied to the coil pairs which are situated along **y**-axis is set to zero instead of I_y and current supplied to the coil pairs situated along **x**-axis is set to I_x instead of zero. In channels with flat surfaces it is possible to change head and tail's position using the T-junction (Fig. 6b).

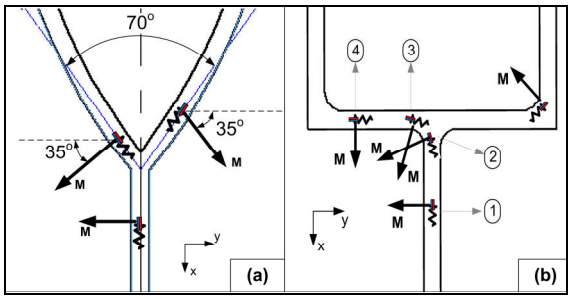

Figure 6. (a) Motion of helical swimmer inside Y-shaped channel. Magnetization of the permanent magnet on the helical swimmer is always perpendicular to the helix axis, and can be directed by changing the direction of the externally applied magnetic field. (b) Motion of helical swimmer inside T-shaped channel. Magnetization of the permanent magnet on the helical swimmer is always perpendicular to the helix axis, and can be directed by changing the direction of the externally applied magnetic field. (1) Current is applied to the coils placed along **y**- and **z**-axis with a phase shift and a negative frequency to move the helical swimmer in negative **x**-direction. (2) Current is applied to the coils placed along **x**-direction having the same phase shift with the ones placed along **y**-direction; though magnetic field vector of **x**-axis coil pairs is smaller than of **y**-axis coil pairs. (3) Reverse situation of (2). (4) Current is applied to the coils placed along **x**- and **z**-axis with a phase shift and a negative frequency to move the helical swimmer in negative **y**-direction.

D. Obstacle Avoiding

The two swimming modes of helical swimmer are also used for avoiding an obstacle inside a rectangular channel. When the swimmer moves forward, it travels along the left hand side of the channel if the rotation frequency is high, and it proceeds to the right hand side as a result of the traction force as soon as the rotation frequency is lowered. The rolling mode of motion is used to change lateral position inside the channel as an alternative to magnetic alignment and navigation so that a possible hindrance can be overcome. In Fig. 7a, schematic representation of this scenario is presented, with the snapshots taken from the experiments for a similar situation (Fig. 7b).

IV. Conclusion

Navigation of helical swimmers inside rectangular channels is demonstrated using magnetic alignment, back and forth motion due to propulsion force and lateral motion due to traction force. With the help of the radially magnetized permanent magnet head, the swimmer is navigated through Y-shaped and T-shaped channels, by changing the rotation axis of the externally applied magnetic field. Controlling the swimming direction by means of changing the direction of externally applied rotating magnetic field is a well studied phenomenon in literature; most of the experimental work on swimming helical micro robots use three pairs of electromagnetic coils to navigate swimmers on a plane or in a volume. In addition to direction control achieved by changing the external magnetic field direction, another mechanism is used to change the swimming direction of swimmers on a plane. It is observed that due to traction forces, magnetic swimmer rolls at lower frequencies, thus lateral motion takes place in addition to the forward motion. Besides basic position control is achieved as well with on-off control mechanism: helical swimmer is driven to the desired place and stopped at a desired location inside Y- and T-shaped channels. With the mentioned swimming modes, it is demonstrated that possible obstacles inside channels and on the way of swimming robots can be overcome during helical robots' travel inside rectangular channels. Future work includes precise position and velocity control of helical swimmer with appropriate sensor systems, e.g. magnetic field sensor, as well as developing a computational fluid

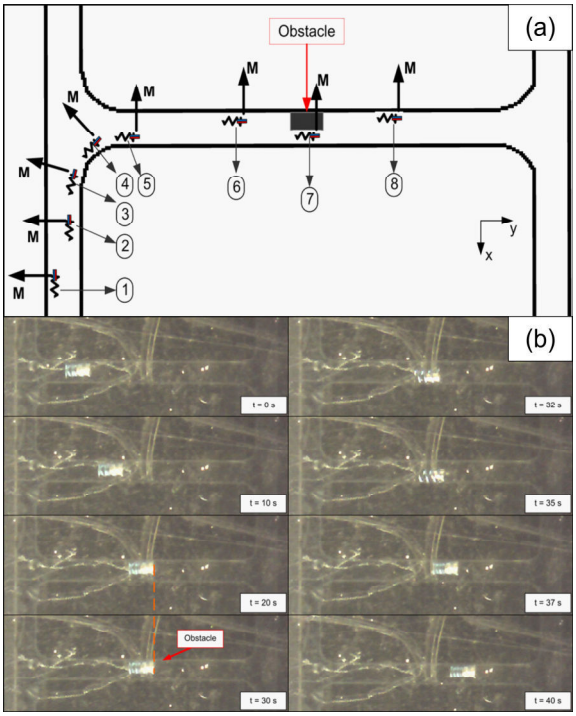

Figure 7. Motion of helical swimmer inside rectangular channel when come across an obstacle. (a) First 5 steps show the magnetic alignment and direction change of helical swimmer as rotational magnetic field changes its direction. (6) Swimmer rotates with 5 Hz and swims forward at the left hand side of the channel. (7) When the motion is interrupted by an obstacle which cannot be moved because of its weight, frequency is decreased to 1 Hz so that traction forces overcome the fluid forces and swimmer proceeds to the right hand side of the channel. (8) As soon as the obstacle avoiding, e.g. robot is placed between obstacle and the channel wall, rotational frequency is increased again for fast forward motion. (b) Forward motion of the helical swimmer placed inside rectangular channel. Rotation frequency is 5 Hz. When t = 20 s swimmer does not move forward although it continues it is rotating at the same frequency. After t = 30 s, the frequency is dropped to 1 Hz and swimmer started to move in lateral direction, thus it avoided the obstacle.

Preprint submitted to 2013 IEEE International Conference on Robotics and Automation. Received September 17, 2012.

dynamics model to investigate fluid forces which cause the direction change in swimming at low or high frequencies.

REFERENCES

[1] B. J. Nelson, I. K. Kaliakatsos, and J. J. Abbott, "Microrobots for minimally invasive medicine," *Annu. Rev. Biomed. Eng*., vol. 12, pp. 55-85, April 2010.

[2] B. Watson, J. Friend, and L. Yeo, "Modeling and testing of a piezoelectric ultrasonic micro-motor suitable for in vivo micro-robotic applications," *Journal of Micromechanics and Microengineering*, vol. 20, pp. 115018-115034, November 2010.

[3] W. Gao, S. Sattayasamitsathit, K. M. Manesh, D. Weihs, and J. Wang, "Magnetically powered flexible metal nanowire motors," *J. Am. Chem. Soc.*, vol. 132, pp. 14403-14405, October 2010.

[4] C. Yu, J. Kim, H. Choi, J. Choi, S. Jeong, K. Cha, J. Park, and S. Park, "Novel electromagnetic actuation system for three-dimensional locomotion and drilling of intravascular microrobot," *Sensors and Actuators A*, vol. 161, pp. 297-304, June 2010.

[5] H. Choi, K. Cha, J. Choi, S. Jeong, S. Jeon, G. Jang, J. Park, and S. Park, "EMA system with gradient and uniform saddle coils for 3D locomotion of microrobot," *Sensors and Actuators A*, vol. 163, pp. 410-417, September 2010.

[6] M. P. Kummer, J. J. Abbott, B. E. Kratochvil, R. Borer, A. Sengul, and B. J. Nelson, "OctoMag: An electromagnetic system for 5-DOF wireless micromanipulation," *IEEE Trans. On Robotics*, vol. 26(6), pp. 1006-1017, December 2010.

[7] T. W. Fountain, P. V. Kailat, and J. J. Abbott, "Wireless control of magnetic helical microrobots using a rotating-permanent magnet manipulator," *IEEE Int. Cong. On Robotics and Automation*, USA, May 2010.

[8] S. H. Kim, S. Hashi, and K. Ishiyama, "Methodology of dynamic actuation for flexible actuator and biomimetic robotics application," *IEEE. Trans. On Magnetics*, vol. 46(6), pp. 1366-1369, June 2010.

[9] T. Okada, S. Guo, and Y. Yamauchi, "A wireless microrobot with 3DOFs in pipe for medical applications," *Proc. of the IEEE/ICME Int. Conf. on Complex Medical Engineering*, China, May 2011.

[10] T. Okada, S. Guo, and Y. Yamauchi, "Design of a wireless hybrid in-pipe microrobot with 3DOFs," *Proc. of the 2011 IEEE Int. Conf on Mechatronics and Automation*, China August 2011.

[11] Q. Pan, S. Huo, and T. Okada, "A novel hybrid wireless microrobot," *Int. J. Mechatronics and Automation*, vol. 1(1), pp. 60-69, March 2011.

[12] J. J. Abbott, K. E. Peyer, M.C. Lagomarsino, L. Zhang, L. Dong, I. K. Kaliakatsos, and B. J. Nelson, "How should microrobots swim?," *The International Journal of Robotics Research*, vol. 28, pp. 1434-1447, November-December 2009.

[13] L. Zhang, J. J. Abbott, L. Dong, et al., "Artificial bacterial flagella: fabrication and magnetic control," *Applied Physics Letters*, vol. 94, pp. 064107-064110, February 2009.

[14] L. Zhang, J. J. Abbott, L. Dong, et al., "Characterization of the swimming properties of artificial bacterial flagella," *Nano Letters*, vol. 9(10), pp. 3663-3667, September 2009.

[15] A. Ghosh and P. Fischer, "Controlled propulsion of artificial magnetic nanostructured propellers," *Nano Letters*, vol. 9 (6), pp. 2243-2245, March 2009.

[16] S. Tottori, L. Zhang, F. Qui, K. K. Krawyck, A. Franco-Obregon, and B. J. Nelson, "Magnetic helical micromachines: fabrication, controlled swimming and cargo transport," *Advanced Materials*, vol. 24, pp. 811-816, February 2012.

[17] S. Schuerle, S. Pane, E. Pellicer, J. Sort, M. D. Baro, and B. J. Nelson, "Helical and tubular lipid microstructures that are electroless-coated with CoNiReP for wirelessmagnetic manipulation," *Small*, vol. 8(10), pp. 1498-1502, May 2012.

[18] Q. Pan, S. Huo, and T. Okada, "Mechanism and control of a spiral type microrobot," *Proc. of the 2010 IEEE Int. Conf. on Information and Automation*, China, June 2010.

[19] S. Jeong, H. Choi, K. Cha, J. Li, J. Park, and S. Park, "Enhanced locomotive and drilling microrobot using precessional and gradient magnetic field," *Sensors and Actuators A*, vol. 171, pp. 429-435, November 2011.

[20] A. W. Mahoney, N. D. Nelson, E. M. Parsons, and J. J. Abbott, "Non-ideal behaviors of magnetically driven screws in soft tissues," *IEEE IROS2012*, unpublished.

[21] T. Honda, K. I. Arai, and K. Ishiyama, "Micro swimming mechanisms propelled by external magnetic fields," *IEEE Trans. On Magnetics*, vol. 32(5), pp. 5085-5087, September 1996.

[22] A. P. Berke, L. Turner, H. C. Berg, and E. Lauga, "Hydrodynamic Attraction of Swimming Microorganisms by Surfaces," *Physical Review Letters*, vol. 101, pp. 038102-, Month 2008.

[23] D. Giacché, T. Ishikawa, and T. Yamaguchi, "Hydrodynamic entrapment of bacteria swimming near a solid surface," *Physical Review E*, vol. 82, pp. 056309-, Month 2010.

[24] F. Z. Temel and S. Yesilyurt, "Magnetically actuated micro swimming of bio-inspired robots in mini channels," *IEEE Int. Conf. on Mechatronics, ICM2011*, Turkey, May 2011.

[25] J. Lighthill, "Flagellar hydrodynamics: the John von Neumann lecture," *SIAM Review*, vol. 18(2), pp. 161-230, April 1976.

[26] L. Arcese, M. Fruchard, and A. Ferreira, "Endovascular magnetically-guidad robots: navigation modeling and optimization," *IEEE Trans. On Biomedical Engineering*, vol. 54(4), pp. 977-987, December 2011.

[27] E. Lauga, W. R. DiLuzio, G. M. Whitesides, and H. A. Stone, "Swimming in circles: motion of bacteria near solid boundaries," *Biophysics Journal*, vol. 90, pp. 400-412, January 2006.